NASA TECHNICAL MEMORANDUM

NASA TM X-52804

NASA TM X-52804

CRITICAL LEVITATION LOCII FOR SPHERES ON CRYOGENIC FLUIDS

by R. C. Hendricks and S. A. Ohm
Lewis Research Center
Cleveland, Ohio

TECHNICAL PAPER proposed for presentation at
Cryogenic Engineering Conference
Boulder, Colorado, June 17-19, 1970

CRITICAL LEVITATION LOCII FOR SPHERES ON CRYOGENIC FLUIDS

by R. C. Hendricks and S. A. Ohm

Lewis Research Center
Cleveland, Ohio

TECHNICAL PAPER proposed for presentation at

Cryogenic Engineering Conference
Boulder, Colorado, June 17-19, 1970

NATIONAL AERONAUTICS AND SPACE ADMINISTRATION

CRITICAL LEVITATION LOCII FOR SPHERES ON CRYOGENIC FLUIDS

by R. C. Hendricks and S. A. Ohm

Lewis Research Center
National Aeronautics and Space Administration
Cleveland, Ohio

ABSTRACT

The forces and governing equations for spheres floating on a fluid of lower specific gravity are examined. Three similarity parameters, Bond number ($Bo = (\rho_l - \rho_v)gR_o^2/g_c$), component density ratio of the sphere to the fluid ($\rho_s - \rho_v/\rho_l - \rho_v$), wetting angle ($\alpha$) and the critical levitation locii, established herein, are sufficient to determine whether or not the sphere will float. Data appear in good agreement with the analysis for a limited range of Bond numbers and a wetting angle of π. These data and the theoretical curve for $\alpha = \pi$ may be approximated by

$$\frac{\rho_s - \rho_v}{\rho_l - \rho_v} = 1.05 + \frac{1.65}{Bo} \qquad 0.1 < Bo < 30$$

Those spheres with density ratios less than this criteria will float, others will sink. More data are needed to verify the analysis over a larger range of Bond numbers and wetting angles.

E-5547

INTRODUCTION

Floating a waxed steel pin on water has long been a source of amusement and an apparent paradox to Archemedes principle. However, a closer examination reveals that one simply has not accounted for all the forces acting to float the pin. A large contribution comes from the effects of surface tension which acts in two ways: first, the free liquid-vapor interface is curved above the solid-liquid-vapor contact line; as such it acts much like a retaining wall, and holds back a fluid head; second, the solid-liquid interfacial tension forces acting on the body are transmitted to the solid-liquid-vapor contact line and held in equilibrium by the free

liquid-vapor interface. An analogy for the latter forces is that of a thin shell tank being supported at the bolting flange.

Beside the usual curiosity of the phenomenon, floating of a noncryogenic fluid on a cryogenic fluid (and vice-versa) is of significant importance in fuel spills (ref. 1). Floatation phenomena are also of interest in studies on controlling hypergolic fires (ref. 2); in the preservation (or destruction) of biological specimens, such as in blood preservation and in enzyme preparation (ref. 3). Floatation phenomena could be of significance in the production of monolayer films, pollution control, and as fundamental tools for the determination of surface wetting characteristics.

The shapes of axisymmetric interfaces have been calculated by Huh and Scriven (ref. 4) and Hendricks and Baumeister (ref. 5).

Huh and Scriven (ref. 4) numerically solved the Laplace capilliary equation, analyzed the errors involved, and presented solution charts and tables for the interface configurations. Hendricks and Baumeister (ref. 5) determined the heat transfer characteristics of a water-sphere floating on a sea of liquid nitrogen in Leidenfrost film boiling. Nutt (ref. 6) examined the forces required to float an isothermal sphere. However, to approximate the submergence depth, Nutt (ref. 6) neglected the curvature along the line of contact and used the closed form solution for a cylinder. Huh and Scriven (ref. 4) found curvature along the line of contact to be important for axisymmetric surfaces at low values of Bond number. While references 4, 5, and 6 deal with the problem of floating spheres and calculating interfaces, only reference 6 gives an approximate criterion for determining if a given isothermal sphere will float on a specified fluid. Such a criterion has not been established for nonisothermal floating spheres and a more accurate solution needs to be established for the isothermal floating spheres. In the ensuing sections we will formulate the governing equations, determine the similarity parameters involved, numerically determine the optimum levitation locii (i.e., a float or no-float criteria) and examine the asymptotic behavior of the solution for both the nonisothermal and isothermal floating spheres. Some experimental data are presented to check the analysis.

THEORETICAL ANALYSIS

In this section we wish to determine the conditions permitting a fluid to support a sphere having a higher specific gravity than its own. The following analysis will produce three basic parameters which together define the maximum floating conditions: Bond number (Bo), that is, the ratio of buoyancy to surface tension forces; the wetting angle of the interface (α)†; and the ratio of solid-liquid specific gravities ($\rho_s - \rho_v / \rho_l - \rho_v$).

We proceed with analysis of the forces at the sphere-liquid interface in order to determine the optimum levitation loci; that is, the conditions permitting floatation of a maximum density sphere. We consider first the force balance on the nonisothermal floating sphere in film boiling (fig. 1(a)), then the force balance on an isothermal sphere (fig. 1(b)), incorporating the work of references 4 and 6. Both cases are subject to the constraint of minimum energy conditions at the interface. A consideration of the limiting cases then defines the asymptotic solutions of the desired loci.

Basic Force Balance for Nonisothermal Sphere

As shown in figure 1(a), the basic model for the nonisothermal floating sphere in film boiling includes a vapor envelope separating the floating sphere and the supporting liquid. This situation occurs, for example, when a water sphere at room temperature (295 K) is placed on saturated liquid nitrogen (77.4 K), and floats on a cushioning layer of nitrogen vapor.

The balance of forces acting to support the sphere, see figure 1(a), may be expressed as:

---

†The value of wetting angle for an advancing interface and that of a receding interface is herein referred to as α, i.e., no distinction is made in the analysis. Thus when using the results, one must use the proper wetting angle; namely, advancing or receding. Also, no allowance for the variation in wetting angle with time is made, although experiments with time dependent values of α (or surface tension σ, or both) could still use the results presented herein by considering time increments.

$$W_s + \int P_v \, dA_1 - \int P_o \, dA_2 - \int \tau_{r\theta} \, dA_3 = 0 \tag{1}$$

where

$$\left.\begin{aligned} dA_1 &= \cos \omega \, R_o^2 \sin \omega \, d\omega \, d\Phi \\ dA_2 &= \cos \theta \, R_o^2 \sin \theta \, d\theta \, d\Phi \\ dA_3 &= \sin \theta \, R_o^2 \sin \theta \, d\theta \, d\Phi \end{aligned}\right\} \tag{2}$$

The pressure in the vapor gap at the sphere surface, P_o, may be expressed in terms of the pressure drop across the vapor gap, ΔP_δ, the pressure drop across the interface, ΔP_σ, and the liquid pressure acting on the interface P_l, see figure 2(a)†.

$$P_o = P_l + \Delta P_\sigma - \Delta P_\delta \tag{3}$$

Using figure 2, the expressions for P_l and P_v become

$$P_v = \left[H_1 + Z_o - R_o(\cos \omega + \cos \theta^*)\right]\rho_v g \tag{4}$$

$$P_l = H_1 \rho_v g + \left[Z_o + (R_o + \delta)(\cos \theta - \cos \theta^*)\right]\rho_l g \tag{5}$$

and because the interface is nearly spherical, the pressure drop across the interface becomes

$$\Delta P_\sigma = \frac{2\sigma}{(R_o + \delta)} \tag{6}$$

The pressure drop across the vapor gap ΔP_δ is determined from equations of reference 5, and equation (4).

---

†The difference in vapor head is quite small and was omitted in ref. 5.

$$\Delta P_\delta = R_o(\rho_l - \rho_v)g\left(p_{\zeta=\varphi} - p_{\zeta=1}\right) + \left(P_{v_{\zeta=\varphi}} - P_{v_{\zeta=1}}\right) = \frac{R_o(\rho_l - \rho_v)gW_s}{\pi w^* f(\theta^*)}$$

$$\times \left(\frac{1 - \varphi^2}{\varphi}\right) + \left[(H_1 + Z_o - R_o \cos\theta^*) - R_o \cos\right]\rho_v g(\varphi^2 - 1) \qquad (7)$$

where

$$\varphi = \frac{1 + \delta}{R_o} \qquad (8)$$

The shear $\tau_{r\theta}$ can be evaluated using the velocity profiles and non-dimensional form of reference 5.

$$\int \tau_{r\theta}\, dA_3 = (1 - \varphi)W_s \qquad (9)$$

Substituting equations (5), (6), and (7) into equation (3) and then substituting equations (2), (3), (4), and (9) into equation (1) gives

$$0 = \varphi W_s + 2\pi \int_0^{\pi-\theta^*} \left[(H_1 + Z_o - R_o \cos\theta^*) - R_o \cos\omega\right]\rho_v g R_o^2 \cos\omega \sin\omega\, d\omega$$

$$- 2\pi \int_0^{\theta^*} \left\{H_1\rho_v g + \frac{2\sigma}{R_o + \delta} + \left[Z_o - (R_o + \delta)\cos\theta^*\right]\rho_l g\right.$$

$$- \frac{R_o(\rho_l - \rho_v)gW_s}{\pi w^* f(\theta^*)}\left(\frac{1 - \varphi^2}{\varphi}\right) - (H_1 + Z_o - R_o\cos\theta^*)\rho_v g(\varphi^2 - 1)$$

$$\left. + \left[R_o\rho_v(\varphi^2 - 1) + (R_o + \delta)\rho_l\right] g\cos\theta\right\} R_o^2 \cos\theta \sin\theta\, d\theta \qquad (10)$$

If the parameters Z_o and θ^* were known, then equation (10) could be integrated in a straight forward manner, (see appendix B) and the force

balance would be complete. However, these parameters must be determined by a simultaneous solution of this force balance and the interface equations, to be found in the theoretical section - Structure of the Interface.

Basic Force Balance for the Isothermal Sphere

As is shown in figure 1(b), the forces in the isothermal sphere-liquid system act directly on the floating sphere. The force balance, equating the weight of the sphere with the buoyancy and surface tension forces, is given by a static force balance analogous to equation (1):

$$W_s - F_B - F_\sigma = 0 \tag{11}$$

Again, the weight of the sphere is,

$$W_s = \frac{4\pi}{3} R_o^3 \rho_s g \tag{12}$$

However, the surface tension forces acting on the sphere are considered to act along the contact circle giving use to the surface tension force, see appendix B,

$$F_\sigma = -\int \sigma_{lv} \sin(\theta^* + \alpha)\, dl$$

$$= -2\pi R_o \sigma_{lv} \sin\theta^* \sin(\theta^* + \alpha) \tag{13}$$

where $dl = R_o \sin\theta^* d\Phi$ over the contact circle. A similar argument is given by Nutt, reference 6.

Appendix C includes a discussion and definition of this surface tension force in terms of adhesive surface tension. The buoyancy force of equation (11) is given by the difference between the supporting liquid force on the liquid-sphere area A_2 and the downward vapor pressure on the vapor-sphere area A_1.

$$F_B = \int_{A_2} P_l \cos\theta \, dA_2 - \int_{A_1} P_v \cos\omega \, dA_1 \qquad (14)$$

where P_v and P_l are defined by equations (4) and (5), see figure 2(b). Again, the buoyancy contribution of equation (14) to the force balance of equation (11) is a matter of simple integration, given the parameters Z_o and θ^*. We now investigate the interface equations in order to solve for these parameters and simplify the force balance in the theoretical section - Force Balance for Both Isothermal and Nonisothermal Levitated Spheres.

Structure of the Interface

In determining the minimum energy configuration of the liquid-vapor interface in both the isothermal and nonisothermal cases, we investigate the forces at the interface, which is considered to be a thin shell as seen in the surface element of figure 3, enlarged in detail AA.† For values of θ greater than θ^*, the interface seeks a minimum energy configuration subject to two constraints: (a) the balance of forces on the sphere at the load circle, and (b) the boundary conditions at ∞. Referring to figure 3, the balance of forces in the X^2-direction becomes:

$$\frac{\partial R_3 N_\tau}{\partial \tau} d\tau \, d\xi - (R_1 N_\xi \, d\xi \, d\tau) \cos(\pi - \tau) + Y_F \, d\tau \, d\xi = 0 \qquad (15)$$

and in the X^3-direction:

$$-R_3 N_\tau \, d\xi \, d\tau + (R_1 N_\xi \, d\tau \, d\xi) \sin(\pi - \tau) + (P_l - P_v) R_3 R_1 \, d\xi \, d\tau = 0 \qquad (16)$$

where N_τ and N_ξ are surface forces per unit length in the ξ and τ directions, respectively. It can be shown that these equations, (15) and (16), represent the governing equations of the liquid interface if

†In ref. 4, Huh and Scriven consider various forms of the interface equations and provide an excellent review of previous works.

$$N_{\xi} = N_{\tau} = \sigma_{l\,v} \tag{17a}$$

and

$$Y_F = 0 \tag{17b}$$

See references (5) and (8). These governing equations may be written as two first-order, nonlinear, ordinary differential equations, subject to equation (17), and reduced to: †

$$D_x u = -\frac{u}{x} - z \tag{18}$$

$$D_x z = \frac{u}{\pm\sqrt{1 - u^2}} = \tan \tau \tag{19}$$

where

$$P_l - P_v = Z(\rho_l - \rho_v)g$$

$$z = \frac{Z}{L} = \frac{Z}{\sqrt{\frac{\sigma_{l\,v}}{(\rho_l - \rho_v)g}}}$$

$$x = \frac{X}{L}$$

$$u = \sin \tau$$

Now, equations (18) and (19) are subject to the boundary conditions:

Sphere load circle. -

$$x = x_o = \sqrt{B\omega} \sin \theta^* \tag{20}$$

$$z = z_o \tag{21}$$

†See refs. 4, 5, and 8.

$$\tau_o = (\pi - \theta^*) + (\pi - \alpha) \tag{22}$$

Interface at ∞. - As $x \to \infty$ (i.e., $x = M >> 0$)

$$z \to 0 \tag{23}$$

$$\tau \to \pi \tag{24}$$

where

$$Bo = \frac{R_o^2}{L^2} = \text{Bond number} \tag{25}$$

The (-) sign in equation (19) is used when $\tau < \pi/2$ and (+) sign used when $\tau > \pi/2$. As the conditions at $\tau = \pi/2$ represents a singularity, this region was handled by changing the independent variable from x to τ.

When $0.93 < u \leq 1$, equations (18) and (19) were rewritten as

$$D_\tau x = -\frac{x \cos \tau}{xz + \sin \tau} \tag{18a}$$

$$D_\tau z = -\frac{x \sin \tau}{xz + \sin \tau} \tag{19a}$$

Details of a more sophisticated and accurate technique are found in reference 4. In either case, a fourth-order Runga-Kutta technique forms the basis of the numerical solution.

Force Balance for Both Isothermal and Nonisothermal Levitated Spheres

For a given Bo and α, the interface equations (18), (19), (18a), and (19a) yield solutions for z_o and θ^*, which can then be used to evaluate either equation (10) or equation (14), thus completing the solutions of equations (1) and (11).

Equation (10) is evaluated in appendix B in a more precise manner than reference 5. For the nonisothermal floater, $\delta/R_o << 1$ which can be demonstrated using the results of reference 5. This implies that

$$\varphi = \left(1 + \frac{\delta}{R_o}\right) \to 1$$

and equation (B10) reduces to an expression in terms of ρ, Bo, and θ^*

$$\frac{2}{3}\left(\frac{\rho_s - \rho_v}{\rho_l - \rho_v}\right) = \sin^2\theta^*\left(\frac{1}{Bo} + \frac{z_o}{2\sqrt{Bo}}\right) + \frac{1}{3} - \frac{\cos^3\theta^*}{3} - \frac{1}{2}\cos\theta^*\sin^2\theta^* \qquad (26)$$

Integration of equation (14), gives for the buoyancy force on the isothermally floating sphere:

$$F_B = 2\pi(\rho_l - \rho_v)gR_o^3\left[\frac{\rho_l + \rho_v}{3(\rho_l - \rho_v)} - \frac{\cos\theta^*}{2} + \frac{\cos^3\theta^*}{6} + \frac{Z_o}{2R_o}(1 - \cos^2\theta^*)\right] \qquad (27)$$

Substituting equation (13) for surface tension force and equation (27) for buoyancy force into equation (11) gives the force balance on the isothermal sphere, expressed in terms of ρ, Bo, θ^*, and α:†

$$\frac{2}{3}\frac{\rho_s - \rho_v}{\rho_l - \rho_v} = \frac{1}{3} - \frac{1}{2}\cos\theta^* + \frac{1}{6}\cos^3\theta^* + \frac{z_o\sin^2\theta^*}{2\sqrt{Bo}} - \frac{\sin\theta^*\sin(\alpha + \theta^*)}{Bo} \qquad (28)$$

Note that equation (26) for the nonisothermal floating sphere is identical to equation (28) for isothermal floater, for $\alpha = \pi$, assuming of course that $\delta/R_o \ll 1$. Thus for the nonisothermal case (film boiling), we can validly employ the maximum floating criteria derived for the isothermal case, with $\alpha = \pi$.

---

†The form of eq. (28) can be altered to agree with that of Huh and Scriven, ref. 4, and is similar to the results of Nutt, ref. 6, within the framework of his assumptions.

Critical Levitation Loci and Asymptotic Limits

In order to obtain graphs of levitation loci as a function of density ratio $(\rho_s + \rho_v/\rho_l - \rho_v)$ over a range of Bond numbers (Bo) for given values of wetting angle (α), we solve equations (18), (19), (18a), and (19a) subject to the boundary conditions, equations (20) through (24) and the constraint equation (28). The solution is obtained by specifying the Bond number, wetting angle, and the θ^* and z_o parameters. Once a fourth order Runga-Kutta solution is attained, the above procedure is repeated for a range of values of θ^* and z_o until the ratio $(\rho_s + \rho_v/\rho_l - \rho_v)$ of equation (28) reaches maximum value. Figure 4(a) presents resulting maximum density ratio loci over Bond number, Bo, values for $\alpha = \pi$, $\pi/2$, and $3\pi/5$ ($3\pi/5$ is for Teflon floating on water); figure 4(b) gives corresponding submergence angles θ^*, and figure 4(c) the corresponding submergence depths z_o, as functions of Bo. For a given Bo and α, spheres with density ratios less than specified by this locus will float; however, spheres with density ratios greater than specified by the locus will not float.

Investigation of the characteristic trends of an equation is both instructive and expedient in determining the desired results. We now investigate the two limiting cases of very large and very small Bond number limits.

As Bond number becomes very large (Bo $\to \infty$) equation (28) is approximated by:

$$\frac{2}{3}\left(\frac{\rho_s + \rho_v}{\rho_l - \rho_v}\right) \approx \frac{1}{3} - \frac{1}{2}\cos\theta^* + \frac{1}{6}\cos^3\theta^* \tag{29}$$

As Bond number becomes quite small, (Bo $\to \epsilon \approx 0$), (i.e., surface tension forces dominate), equation (28) becomes

$$\frac{2}{3}\left(\frac{\rho_s + \rho_v}{\rho_l - \rho_v}\right) \approx \frac{z_o \sin^2\theta^*}{2\sqrt{\text{Bo}}} - \frac{\sin\theta^* \sin(\theta^* + \alpha)}{\text{Bo}} \tag{30}$$

$$\frac{2}{3}\left(\frac{\rho_s + \rho_v}{\rho_l - \rho_v}\right) \simeq -\frac{\sin\theta^* \sin(\theta^* + \alpha)}{\text{Bo}} \tag{31}$$

The expected asymptotic behavior of the critical Levitation Locii as determined from equations (29) and (31) is summarized in table I.

The asymptotic limits established in this section are in good agreement with the computed locii, and establish the trends for the limits of low and high Bond numbers (see fig. 4).

RESULTS AND DISCUSSION

A number of solid and liquid spheres have been floated on water and liquid nitrogen, respectively, to test the Optimum Levitation Locii of figure 4. The solid teflon spheres and fluid containers were carefully cleaned prior to attempting to float a given sphere in the isothermal state. The spheres were then placed on the supporting fluid with tweezers. While this technique is satisfactory for these experiments, more precisely controlled experiments will require a sting or comparable type support in conjunction with an analytical balance. In the experiments of Nutt (ref. 6) a centrifuge was employed to vary the local acceleration and give first order results; however while the technique is a good one, a larger container should be employed to minimize the effects of curvature at the container wall. The liquid spheres were formed using a hypodermic needle, squeezed out and carefully dripped onto the liquid nitrogen surface (the nonisothermal state). While this technique is adequate for our case, more accurate data will require a technique which can minimize the surface impact. The size of the frozen spheres were measured by comparison to teflon spheres and checked using a scale.

To determine if a given material would float on a specific fluid, various diameter spheres were tried. Sphere diameter was increased until the surface could no longer support the sphere and it sank. In most cases, the graduations in sphere diameter were too coarse to permit the determination of the critical size. These "largest size" levitated sphere data are presented in table II and figure 4(a).

The data for $\alpha = \pi$ (i.e., those spheres floating on liquid nitrogen) are in good agreement with the theoretical line for a limited range of Bond number. The teflon sphere data, $\alpha \approx 3\pi/5$, also appear to be in good agreement with the analysis.

To illustrate the sensitivity of the data, a 0.31 centimeter diameter carbon tetrachloride sphere would float momentarily on liquid nitrogen and sink to the bottom while a 0.28 centimeter sphere floated. Carbon tetrachloride spheres 0.31 centimeter diameter and above are classified as nonfloaters on liquid nitrogen. A 0.635 centimeter diameter teflon sphere would not float on water while other teflon spheres (0.318, 0.397, and 0.476 cm diam.) would float on water.

From these results it appears that the parameters of Bond number ($Bo = \left[(\rho_l - \rho_v)gR_Q^2\right]/\sigma g_c$), density ratio ($\rho_s - \rho_v/\rho_l - \rho_v$), and the wetting angle (α) used in conjunction with figure 4 are sufficient to predict whether or not a given sphere will float on a specified fluid. A decrease in the wetting angle (increased wetting which effects the surface tension support) while holding Bond number constant will affect a decrease in the density ratio ($\rho_s - \rho_v/\rho_l - \rho_v$); this means that a less dense sphere can be supported. It is apparent from figure 4 and the data that the effects of α become more significant at low Bond numbers, and a contaminated surface will greatly alter the results. As a more specific example, teflon spheres of diameter greater than 0.318 centimeter would not float as received from the manufacturer. However, degreasing and cleaning the surface resulted in good agreement with the optimum levitation locus for teflon on water.

The effects of advancing and receding wetting angle, α, have been incorporated in the analysis because the α-parametric curves of figures 4(a) and (b) represent either value of α. The time dependency of α has not been incorporated; however, if the values of α are known as a function of time, figures 4(a) and (b) should give good results. The solutions should also be valid for temperature variations in surface tension σ_{lv} of the supporting fluid provided the heating rates are not large or the fluid near its thermodynamic critical point (i.e., the sphere and the liquid remain close to isothermal and heat transfer is very small). If this premise is violated then the governing equations must include heat transfer.

Bond number appears to be the most easily controlled parameter and, as it characterizes the supporting liquid interface, becomes the fundamental independent variable in the experiments (e.g., the size of the sphere was

changed in our experiments and acceleration was the variable in the experiments of Nutt (ref. 6)); the value of $\sigma_{l,v}$ could be changed by heating the fluid. Where the Bond number is changed by changing sphere size, the values of θ^* and z_o can be estimated by the technique presented in appendix D. Other fluids and solids need to be examined to determine the range of validity of the analysis.

CONCLUSIONS

The forces and associated governing equations for isothermal and non-isothermal spheres (film boiling) floating on a fluid of lower specific gravity have been examined. Criteris for floating spheres called the Critical Levitation Locii have been established. Bond number $Bo = \left[(\rho_l - \rho_v)gR_o^2\right]/\sigma g_c$; density ratio, $(\rho_s - \rho_v/\rho_l - \rho_v)$; wetting angle, α; used in conjunction with figure 4 appear to be sufficient to determine if a given sphere will float on a specified fluid. For the case of $\alpha = \pi$ the Critical Levitation Locus may be approximated by:

$$\frac{\rho_s - \rho_v}{\rho_l - \rho_v} = 1.05 + \frac{1.65}{Bo} \qquad 0.1 < Bo < 30$$

Data for glycerine, carbon tetrachloride, and water spheres floating on a sea of liquid nitrogen appear to be in good agreement with the analysis. Data for teflon spheres on water also appear to be in agreement with the analytical results.

More exact and extensive measurements are required to determine the validity of the Critical Levitation Locii over a range of Bond numbers (Bo) and wetting angles (α).

The effects of wetting angle, surface tension, and their time, temperature dependencies bear further investigation.

APPENDIX A

SYMBOLS

A	area, cm^2
A_o	parametric form defined by eq. (B2)
A_1	$\left[R_3 + (\partial R_3/\partial\tau)\, d\tau\right] d\xi \left[N_\tau + (\partial N_\tau/\partial\tau)\, d\tau\right]$, see fig. 3
B	parametric form defined by eq. (B3)
Bo	Bond number, $(\rho_l - \rho_v)gR_o^2/\sigma g_c$
F_B	lift force due to buoyancy, dyne
F_σ	lift force due to surface tension, dyne
$f(\theta^*)$	functional form in eqs. (7) and (10), $\cos^2\theta^* - 2\cos\theta^* + 1$
g	local acceleration of gravity, cm/sec^2
g_c	gravitational conversion constant, $1\left[(g)(cm)/(dyne)(sec^2)\right]$
H_1	arbitrary reference pressure head, cm
h_1	arbitrary reference dimensionless pressure head, H_1/L
L	reference length, $\sqrt{\sigma_{lv} g_c/(\rho_l - \rho_v)g}$ cm
M	a large positive number
N	surface force per unit length, dyne/cm
P	pressure, dimensional; $dyne/cm^2$
P_o	pressure acting on the sphere within the vapor gap, $dyne/cm^2$
P_φ	pressure acting on the interface from within the vapor gap, $dyne/cm^2$
ΔP_σ	pressure drop across the liquid vapor interface, $dyne/cm^2$
ΔP_δ	pressure drop across the vapor gap, $dyne/cm^2$
p	pressure, dimensionless
R_o	sphere radius, cm

R_1, R_2	Gaussian radii of curvature, cm
R_3	radius defined in fig. 3(b)
r	radial coordinate, cm
u	dependent variable of eq. (18), sin τ
u*	reference velocity, ν/R_o cm/sec
W_s	weight of the sphere, dyne
w*	reference weight, $\rho u^{*2} R_o^2/g_c$ dyne
X	horizontal coordinate, dimensional; cm
X^1, X^2, X^3	coordinate system, fig. 3(b)
x	dimensionless horizontal coordinate, X/L
Y_F	force tangent to the surface, dyne
Z	pressure head, dimensional; cm
z	dimensionless pressure head, Z/L
α	wetting angle, radians
δ	vapor gap thickness, cm
ϵ	a small positive number
ζ	dimensionless radial coordinate, r/R_o
θ	angular coordinate, rad
θ^*	angle to which the sphere is submerged, rad
ν	kinematic viscosity, cm^2/sec
ρ	density, g/cm^3
σ	surface tension, dynes/cm
τ	angular coordinate, radians
ϕ	angular coordinate, rad

φ dimensionless gap coordinate, $1 + \delta/R_o$

Φ aximuthal coordinate, rad

ξ angular coordinate, radians

Subscripts:

adh adhesion

cr critical

l liquid

lv liquid-vapor

s sphere

sl solid-liquid

sv solid-vapor

v vapor

0 initial

1,2,3 reference conditions

τ, ξ in the direction these angular coordinates

APPENDIX B

SOLUTION OF THE FORCE BALANCE

In this appendix, equation (10) is integrated and reduced to nondimensional form.

Assuming that the parameters Z_o and θ^* have been determined elsewhere, the antiderivative of equation (10) becomes:

$$0 = \frac{W_s \varphi}{2\pi} + A_o \rho_v g R_o^2 \left(\frac{-\cos^2 \omega}{2}\right)\Bigg|_0^{\pi-\theta^*} - R_o^3 \rho_v g \left(\frac{-\cos^3 \omega}{3}\right)\Bigg|_0^{\pi-\theta^*}$$

$$-BR_o^2 \left(\frac{-\cos^2 \theta}{2}\right)\Bigg|_0^{\theta^*} - \left\{(R_o + \delta)\rho_l - \rho_v\left[\left(1 + \frac{\delta}{R_o}\right)^2 - 1\right] R_o\right\}$$

$$\times g \left(\frac{-\cos^3 \theta^*}{3}\right)\Bigg|_0^{\theta^*} \tag{B1}$$

where

$$A_o \equiv H_1 + Z_o - R_o \cos \theta^* \tag{B2}$$

$$B \equiv H_1 \rho_v g + \frac{2\sigma}{R_o + \delta} + \left[Z_o - (R_o + \delta) \cos \theta^*\right]\rho_l g$$

$$- \frac{R_o(\rho_l - \rho_v) g W_s}{\pi w^* f(\theta^*)} \left(\frac{1 - \varphi^2}{\varphi}\right) - \rho_v g \left[\left(1 + \frac{\delta}{R_o}\right)^2 - 1\right] A_o \tag{B3}$$

Evaluating (B1) gives

$$0 = \frac{W_s\varphi}{2\pi} + R_o^2\left(\frac{1 - \cos^2\theta^*}{2}\right)(A_o\rho_v g - B) - R_o^3\rho_v g\left(\frac{\cos^3\theta^* + 1}{3}\right)$$

$$+ \left[(R_o + \delta)\rho\ g - \rho_v g(\varphi^2 - 1)R_o\right]R_o^2\left(\frac{\cos^3\theta^* - 1}{3}\right) \qquad \text{(B4)}$$

$$0 = \frac{W_s\varphi}{2\pi} - \frac{R_o^3 g}{3}\left(1 + \frac{\delta}{R_o}\right)\left[\rho_v\left(1 + \frac{\delta}{R_o}\right) + \rho_l\right] + \frac{\cos^3\theta^*}{3}R_o^3 g\left\{\left(1 + \frac{\delta}{R_o}\right)\rho_l\right.$$

$$\left. - \left[2 - \left(1 + \frac{\delta}{R_o}\right)^2\right]\rho_v\right\} - \frac{R_o^2\sin^2\theta^*}{2}\left[-H_1\rho_v g - Z_o\rho_v g\left(1 + \frac{\delta}{R_o}\right)^2\right.$$

$$+ R_o\cos\theta^*\rho_v g\left(1 + \frac{\delta}{R_o}\right)^2 + H_1\rho_v g\left(1 + \frac{\delta}{R_o}\right)^2 - \frac{2\sigma}{R_o + \delta} + Z_o\rho_l g$$

$$\left. - R_o\left(1 + \frac{\delta}{R_o}\right)\cos\theta^*\rho_l g - \frac{R_o(\rho_l - \rho_v)gW_s(1 - \varphi^2)}{\pi w^* f(\theta^*)\varphi}\right] \qquad \text{(B5)}$$

Regrouping the terms of equation (B5)

$$0 = \frac{W_s\varphi}{2\pi} - \frac{R_o^3 g\varphi}{3}(\rho_v\varphi + \rho_l) + \frac{\cos^3\theta^*}{3}R_o^3 g\left[\rho_l\varphi - (2 - \varphi^2)\rho_v\right]$$

$$- \frac{R_o^2\sin^2\theta^*}{2}\left\{H_1\rho_v g(1 - \varphi^2) - Z_o g(\rho_v\varphi^2 - \rho_l) + \frac{2\sigma}{R_o\varphi}\right.$$

$$\left. - \cos\theta^* g\left[(R_o + \delta)\rho_l - R_o\varphi^2\rho_v\right] - \frac{R_o(\rho_l - \rho_v)gW_s}{\pi w^* f(\theta^*)}\left(\frac{1 - \varphi^2}{\varphi}\right)\right\} \qquad \text{(B6)}$$

Collecting terms of (B6) and dividing by $(\rho_l - \rho_v)gR_o^3$,

$$0 = \frac{W_s\varphi}{2\pi(\rho_l - \rho_v)gR_o^3} - \frac{\varphi}{3}\left(\frac{\rho_l + \rho_v\varphi}{\rho_l + \rho_v}\right) + \frac{\cos^3\theta^*}{3}\left[\frac{\rho_l\varphi - (2 - \varphi^2)\rho_v}{\rho_l - \rho_v}\right]$$

$$- \frac{H_1}{R_o}\frac{\rho_v}{\rho_l - \rho_v}\left(\frac{1 - \varphi^2}{2}\right)\sin^2\theta^* + \frac{Z_o}{2R_o}\left(\frac{\rho_v\varphi^2 - \rho_l}{\rho_l - \rho_v}\right)\sin^2\theta^*$$

$$- \frac{\sigma\sin^2\theta^*}{(\rho_l - \rho_v)gR_o^2\varphi} + \frac{\varphi\cos\theta^*\sin^2\theta^*}{2}\left(\frac{\rho_l - \rho_v\varphi}{\rho_l - \rho_v}\right)$$

$$+ \frac{W_s(1 - \varphi^2)}{\pi w^* f(\theta^*)}\frac{\sin^2\theta^*}{2\varphi} \qquad \text{(B7)}$$

Introducing Bond number

$$Bo = \frac{(\rho_l - \rho_v)gR_o^2}{\sigma} = \frac{R_o^2}{L^2} \qquad (26)$$

equation (B7) becomes:

$$0 = \frac{2\rho_s\varphi}{3(\rho_l - \rho_v)} - \frac{\varphi}{3}\left(\frac{\rho_l + \rho_v\varphi}{\rho_l - \rho_v}\right) + \frac{\cos^3\theta^*}{3}\left[\frac{\rho_l - (2 - \varphi^2)\rho_v}{\rho_l - \rho_v}\right]$$

$$+ \frac{\cos\theta^*\sin^2\theta^*}{2}\varphi\left(\frac{\rho_l - \rho_v\varphi}{\rho_l - \rho_v}\right) - \frac{z_o\sin^2\theta^*}{2\sqrt{Bo}}\left(\frac{\rho_l - \rho_v\varphi^2}{\rho_l - \rho_v}\right)$$

$$- \frac{\sin^2\theta^*}{\varphi Bo} - \left[\frac{h_1\varphi}{\sqrt{Bo}}\left(\frac{\rho_v}{\rho_l - \rho_v}\right) - \frac{W_s}{\pi w^* f(\theta^*)}\right]\left(\frac{1 - \varphi^2}{2\varphi}\right)\sin^2\theta^* \qquad \text{(B8)}$$

Regrouping, the density ratios of equation (B8)

$$\frac{2\rho_s\varphi}{3(\rho_l - \rho_v)} - \frac{\varphi}{3}\left(\frac{\rho_l + \rho_v\varphi}{\rho_l - \rho_v}\right) + \frac{1}{3} - \frac{1}{3} = \frac{2\rho_s\varphi - \rho_l\varphi - \rho_v\varphi^2 + \rho_l - \rho_v}{3(\rho_l - \rho_v)} - \frac{1}{3}$$

$$= \frac{\left[2\varphi\rho_s - (1 + \varphi^2)\rho_v\right] + \rho_l(1 - \varphi)}{3(\rho_l - \rho_v)} - \frac{1}{3} \qquad \text{(B9)}$$

And finally substituting equation (B9) into (B8), equation (B8) reduces to

$$\frac{\left[2\varphi\rho_s - (1 + \varphi^2)\rho_v\right] + \rho_l(1 - \varphi)}{3(\rho_l - \rho_v)} = \frac{1}{3} - \frac{\cos\theta^* \sin^2\theta^*}{2}\left[\frac{\rho_l - (2 - \varphi^2)\rho_v}{\rho_l - \rho_v}\right]$$

$$- \frac{\cos^3\theta^*}{3}\varphi\left(\frac{\rho_l - \rho_v\varphi}{\rho_l - \rho_v}\right) + \sin^2\theta^*\left[\frac{1}{\varphi Bo} + \frac{z_o}{2\sqrt{Bo}}\left(\frac{\rho_l - \rho_v\varphi^2}{\rho_l - \rho_v}\right)\right]$$

$$+ \left[\frac{h_1\varphi}{\sqrt{Bo}}\left(\frac{\rho_v}{\rho_l - \rho_v}\right) - \frac{W_s}{\pi w^* f(\theta^*)}\right]\left(\frac{1 - \varphi^2}{2\varphi}\right)\sin^2\theta^* \qquad \text{(B10)}$$

APPENDIX C

SURFACE TENSION SUPPORT (ISOTHERMAL-SPHERE)

If a load is placed on an axisymmetric shell or membrane structure, it is in effect transmitted to a contact circle. In our case this contact circle is represented by the liquid-vapor-solid, or fluid A-fluid B-solid interface. The surface forces acting at this interface are illustrated in figure 3.

While surface tension, σ_{lv}, and the wetting angle α characterize the interface, it is useful to think of surface forces in vector terminology.

The components of surface tension acting to support the sphere and those tending to pull the sphere into the liquid are illustrated in figure 5. If we define the adhesive tension at the contact circle to be σ_{adh}, which acts normal to the surface, then a balance of forces requires that

$$\sigma_{adh} = \sigma_{lv} \sin \alpha \tag{C1}$$

As the horizontal forces are balanced because of symmetry, vertical upward force, F_σ, balances the vertical downward forces:

$$0 = F_\sigma - 2\pi R_o \sin \theta^* (-\sigma_{adh} \cos \theta^* + \sigma_{sl} \sin \theta^* - \sigma_{sv} \sin \theta^*) \tag{C2}$$

where $2\pi R_o \sin \theta^*$ is the circumference of the contact circle. But the Young-Duprè equation gives

$$\sigma_{lv} \cos \alpha + \sigma_{sl} = \sigma_{sv} \tag{C3}$$

and upon substitution of equations (C1) and (C3), equation (C2) becomes

$$F_\sigma = -2\pi R_o \sigma_{lv} \sin \theta^* \sin (\theta^* + \alpha) \tag{C4}$$

Equation (C4) also results from assuming that σ_{lv} and α completely characterize the interface. Resolving σ_{lv}, the vertical component becomes,

$$\sigma_{lv} \cos \left(\theta^* + \alpha\right) - \frac{3\pi}{2} = -\sigma_{lv} \sin (\theta^* + \alpha) \tag{C5}$$

and integrating equation (C5) over the contact circle gives equation (C4).

APPENDIX D

ESTIMATING θ^* FOR NONOPTIMUM FLOATER

Enter figure 4(a) with the density ratio $\left[(\rho_s - \rho_v)/(\rho_l - \rho_v)\right]_1$ and α; determine the critical Bond number Bo_{cr_1}. If we assume that the Bond number change is effected by a change in R_o, then estimate a new density ratio

$$\left(\frac{\rho_s - \rho_v}{\rho_l - \rho_v}\right)_2 = \left(\frac{\rho_s - \rho_v}{\rho_l - \rho_v}\right)_1 \frac{R_{o,1}^3}{\left[\dfrac{\sigma Bo_{cr_1}}{(\rho_l - \rho_v)g}\right]^{3/2}} \tag{D1}$$

Re-enter figure 4 with $\left[(\rho_s - \rho_v)/(\rho_l - \rho_v)\right]_2$ and α and determine a new critical Bond number Bo_{cr_2}. Using Bo_{cr_2} find θ^*, and z_o from figures 4(b) and (c), respectively. The technique appears to be valid for small changes in Bond number.

REFERENCES

1. Anon.: Propellant Work Shows New Film Boiling Aspect. Chem. Eng. News, vol. 44, no. 17, Apr. 25, 1966, pp. 58-61.
2. Apollo Land Rescue Team (private communication).
3. Dr. Arthur P. Rinfret (private communication).
4. Huh, Chun; and Scriven, L. E.: Shapes of Axisymmetric Fluid Interfaces of Unbounded Extent. J. Colloid Interface Sci., vol. 30, no. 3, July 1969, pp. 323-337.
5. Hendricks, Robert C.; and Baumeister, Kenneth J.: Heat Transfer and Levitation of a Sphere in Leidenfrost Boiling. Proposed NASA Technical Note.
6. Nutt, C. W.: Froth floatation: The Adhesion of Solid Particles to Flat Interfaces and Bubbles. Chem. Eng. Sci., vol. 12, 1960, pp. 133-141.
7. Reynolds, William C.; and Satterlee, Hugh M.: Liquid Propellant Behavior at Low and Zero G. The Dynamic Behavior of Liquids in Moving Containers. H. Norman Abramson, ed. NASA SP-106, 1966, pp. 387-449.
8. Timoshenko, S.; Woinowsky-Krieger, S.: Theory of Plates and Shells. Second ed., McGraw-Hill Book Co., Inc., 1959, pp. 443-445.

TABLE I. - SOME EXPECTED ASYMPTOTIC BEHAVIOR OF THE CRITICAL LEVITATION LOCII

Bond number	Density ratio and θ^*	
$Bo \to \epsilon \approx 0$	$\alpha \to \pi$	$\frac{\rho_s - \rho_v}{\rho_l - \rho_v} \to \frac{3}{2Bo}$ $\theta^* \to \frac{\pi}{2}$
	$\alpha \to \frac{\pi}{2}$	$\frac{\rho_s - \rho_v}{\rho_l - \rho_v} \to \frac{3}{4Bo}$ $\theta^* \to \frac{3\pi}{4}$
$Bo \to \infty$	$\frac{\rho_s - \rho_v}{\rho_l - \rho_v} \to 1$ $\theta^* \to \pi$	
For all Bo $\alpha \to 0$	$\frac{\rho_s - \rho_v}{\rho_l - \rho_v} \to 1$ $\theta^* \to \pi$	

TABLE II. - LEVITATED SPHERE DATA FOR A VARIETY OF SPHERES AND SUPPORTING FLUIDS

Sphere		State	Supporting fluid				Maximum diameter sphere floated, cm
Material	Density, g/cc		Material	Density, g/cc	In contrast with the fluid	Wetting angle, radians	
Teflon	2.14	Isothermal	Water	1.0	Air	$3\pi/5$	0.476
Carbon-tetrachloride	1.585	Nonisothermal	Liquid nitrogen	0.8	Air and nitrogen vapor	π	0.28
Glycerine	1.25	Nonisothermal	Liquid nitrogen	0.8	Air and nitrogen vapor	π	0.335
Water	1.0	Nonisothermal	Liquid nitrogen	0.8	Air and nitrogen vapor	π	0.63

$$W_s + \int P_v \cos\omega \, dA_1 - \int P_0 \cos\theta \, dA_2 - \int \tau_{r\theta} \sin\theta \, dA_2 = 0$$

$$W_s + \int P_v \cos\omega \, dA_1 - \int P_\ell \cos\theta \, dA_2 - \oint \sigma_{LV} \sin(\theta^* + \alpha) d\ell = 0$$

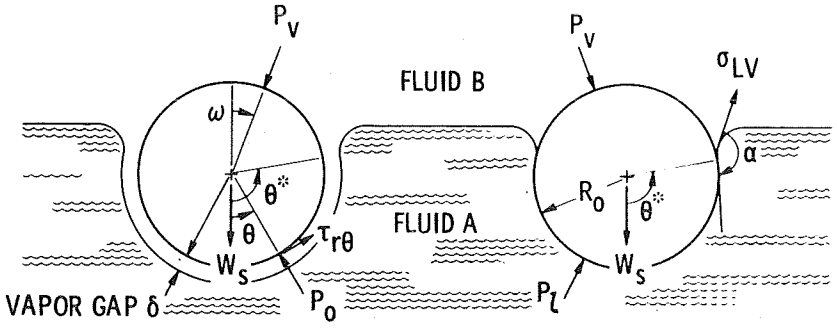

(A) FORCES ACTING ON THE NON-ISOTHERMAL FLOATING-SPHERE IN FILM BOILING.

(B) FORCES ACTING ON THE ISOTHERMAL FLOATING-SPHERE.

Figure 1. - Free body force balance for levitated spheres.

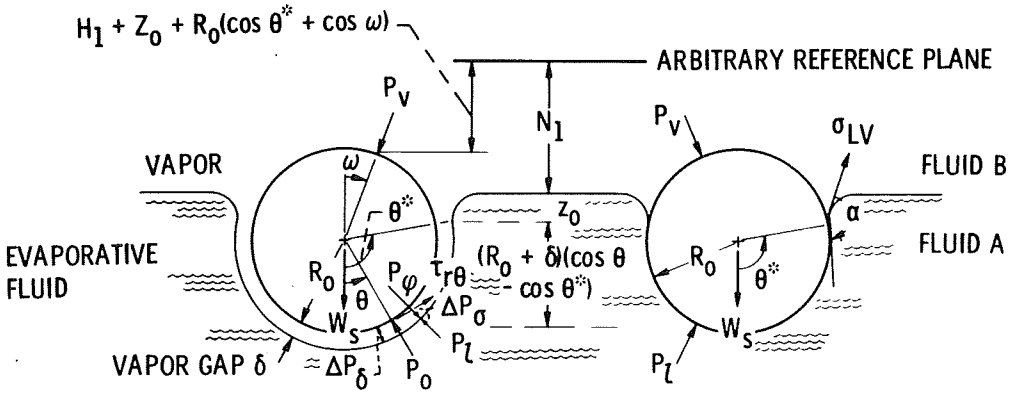

(A) THE NONISOTHERMAL FLOATING-SPHERE IN FILM BOILING.

(B) THE ISOTHERMAL FLOATING-SPHERE.

Figure 2. - Detailed force analysis of floating spheres.

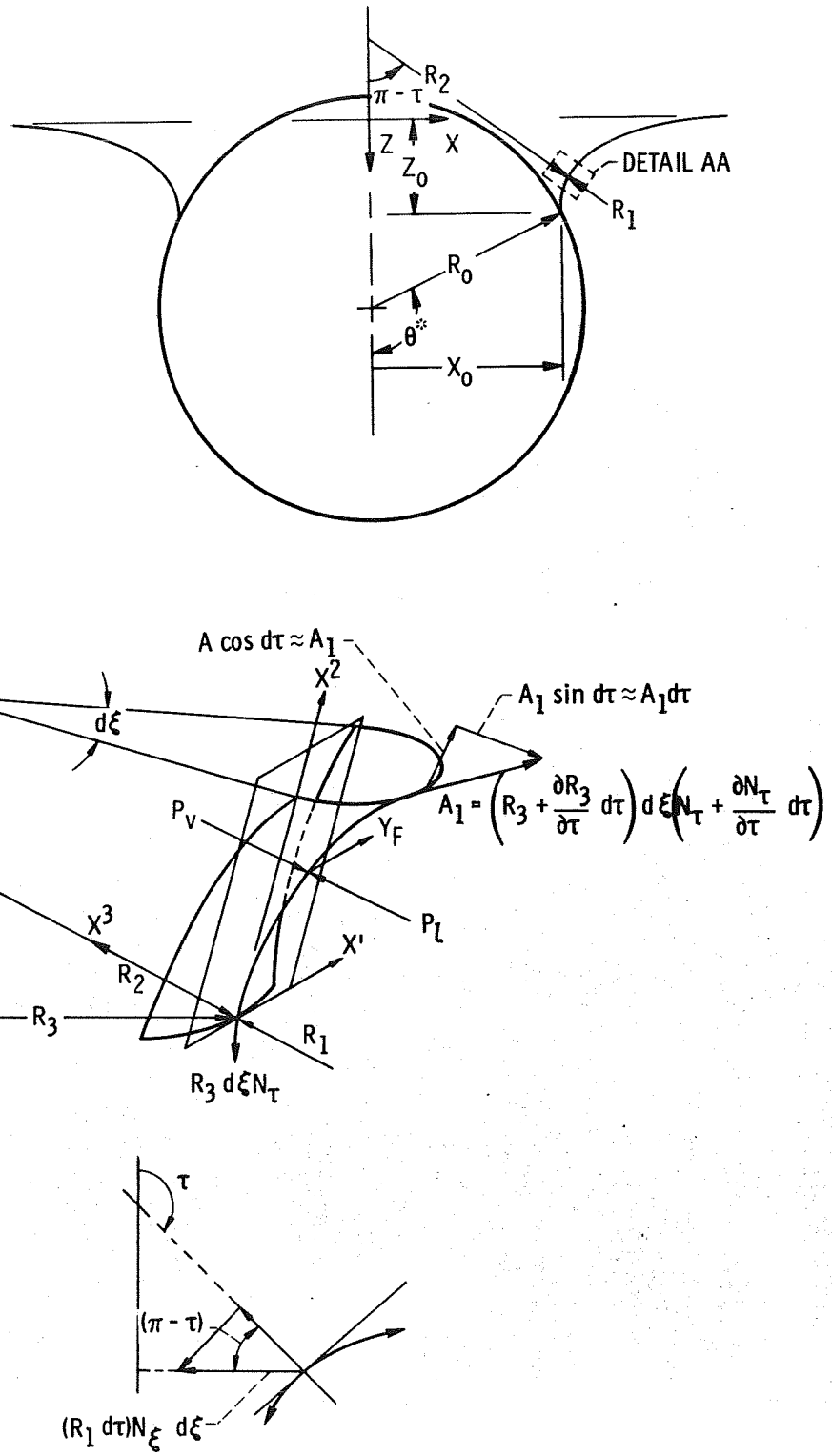

Figure 3. - Forces acting on a "thin shell" section of the vapor-liquid interface.

		FLUID SPHERE	α
○	FLOAT	WATER	
□	FLOAT	ETHYLENE GLYCOL	π
□	NO FLOAT		
△	FLOAT	GLYCERINE	π
△	NO FLOAT		
▷	FLOAT	CARBONTETRA-CHLORIDE	π
▷	NO FLOAT		
⬠	FLOAT	TEFLON ON WATER	3π/5
◇	NO FLOAT	ISOTHERMAL	

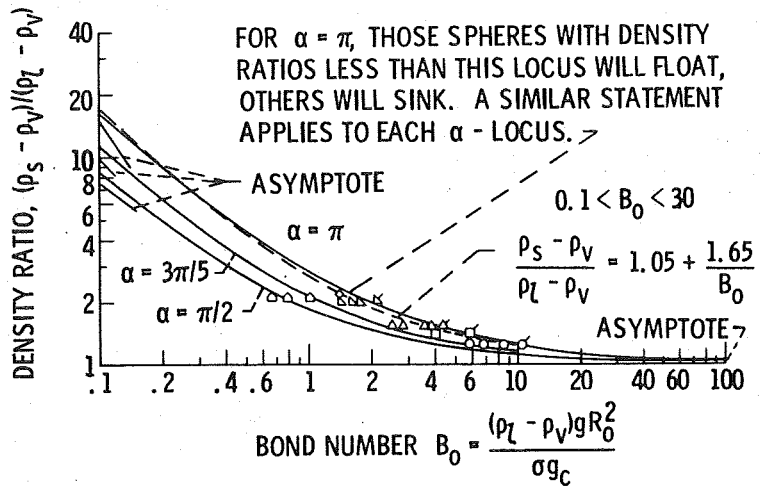

Figure 4(a). - A comparison of the critical levitation locus and various floating spheres on liquid nitrogen. (A Teflon sphere floating on water is included for comparison.)

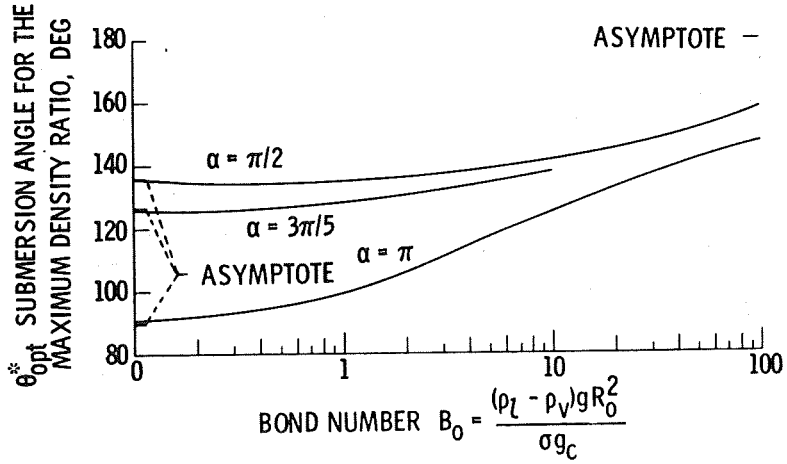

Figure 4(b). - Submersion angle θ^*_{opt} for the optimum density ratio.

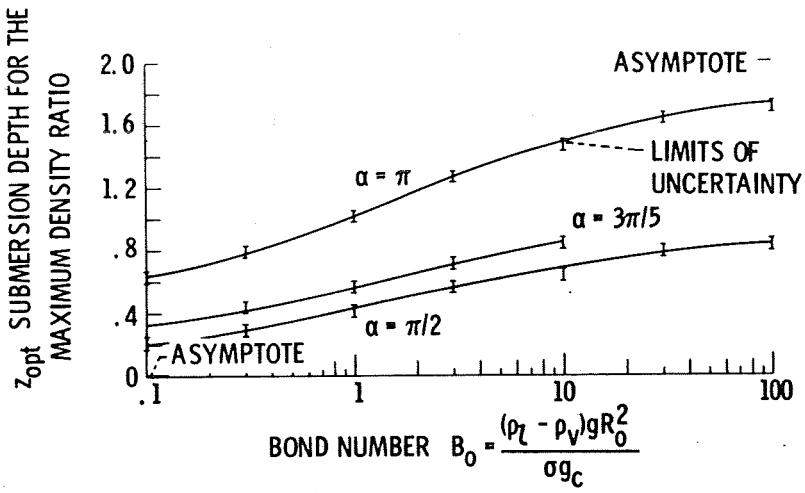

Figure 4(c). - Submersion depth z_0 for the optimum density ratio.

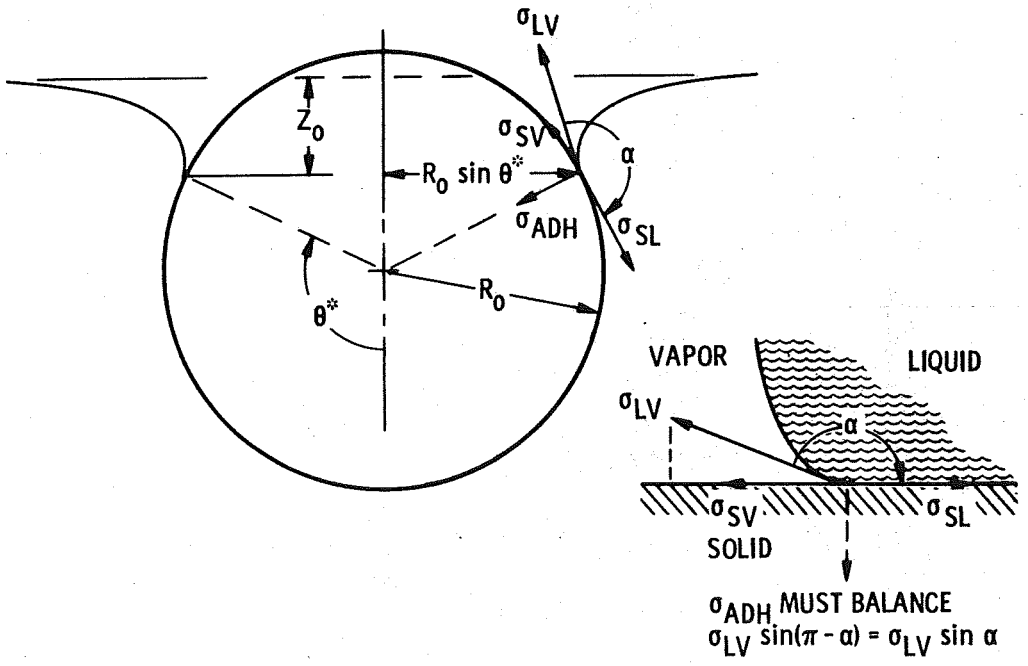

Figure 5. - Surface forces acting at the contact circle.